

## Identification of the Short-Range Intramolecular Excimers in Polyacenaphthalene

Francisco Mendicuti, Rekha Kulkarni, Bharat Patel, and Wayne L. Mattice\*

*Departamento de Quimica Fisica, Universidad de Alcala de Henares, Alcala de Henares, Madrid, Spain, and Department of Polymer Science, The University of Akron, Akron, Ohio 44325-3909. Received October 2, 1989;  
Revised Manuscript Received November 27, 1989*

**ABSTRACT:** Molecular modeling has been used to search for conformations conducive to formation of a singlet excimer between naphthalene rings on units  $i$  and  $i + j$ , for  $j = 1-5$ , in polyacenaphthalene. For appropriate stereochemical compositions, such conformations can be found for  $j = 1$  or  $2$ , but no such conformations were found for  $j = 3-5$ . The difference in the relative intensity of the fluorescence from the excimer and from the monomer in polyacenaphthalene samples with different stereochemical compositions can be rationalized by an analysis that utilizes the excimers with  $j = 1$  and  $j = 2$ . This analysis would fail if the nearest-neighbor excimers were arbitrarily excluded.

### Introduction

It has been well established that dilute solutions of polyacenaphthalene exhibit fluorescence from both the monomer and the excimer.<sup>1-5</sup> The ratio of the intensities of fluorescence from the excimer and monomer, denoted by  $I_D/I_M$ , depends on the stereochemical composition of the polymer.<sup>4</sup> The decays of the fluorescence from the excimer and monomer cannot be analyzed with the conventional kinetic scheme that leads to a sum and difference of exponentials but instead requires three exponentials.<sup>5</sup> The origin of the excimer emission has commonly been attributed to the formation of an excited complex between next-to-nearest neighbor naphthalene groups.<sup>2-6</sup> The basis for the exclusion of the possibility of the formation of an excimer by naphthalene groups that are nearest neighbors appears to have been the difficulty in making a planar sandwich<sup>7</sup> with molecular models of the diads.<sup>2-6</sup>

The purpose here is to present experimental results and molecular modeling that argue for a modification of the accepted picture of the formation of intramolecular excimers in polyacenaphthalene. These results support the identification of next-to-nearest neighbor naphthalene groups as being important contributors to the excimer emission, but they also strongly implicate naphthalene groups that are nearest neighbors in the formation of excimer.

### Experimental Section

Acenaphthene was purchased from Aldrich. One sample of polyacenaphthalene was prepared by cationic polymerization in solution, and the other sample was prepared by thermal polymerization in the bulk.<sup>8,9</sup> The weight-average molecular weights, as determined by using gel permeation chromatography, were 18 000 and 120 000, respectively. Excimer formation in polyacenaphthalene has been shown to be insensitive to molecular weight, except that it does not take place near the ends in polymers prepared by cationic polymerization.<sup>4</sup> The stereochemical compositions, as determined by nuclear magnetic resonance, infrared, and ultraviolet spectroscopies, are predominantly threeo-diisotactic for the polymer prepared by cationic polymerization in solution, and threeo-disyndiotactic for the polymer prepared in the bulk.<sup>10</sup> The nomenclature for the stereochemical compositions is that of Huggins et al.<sup>11</sup> Idealized conformations of hexamers with each of these stereochemical compositions are depicted in Figure 1.

Fluorescence measurements were performed with an SLM 8000C fluorometer equipped with a double excitation monochromator. Polarizers in the excitation and emission paths were set for magic-angle conditions. Slits were 8 nm for excitation and 4 nm for emission. Typical optical densities at the wavelength of excitation were in the range 0.05-0.1. Emission spectra were not corrected for the wavelength dependence of the instrumental response.

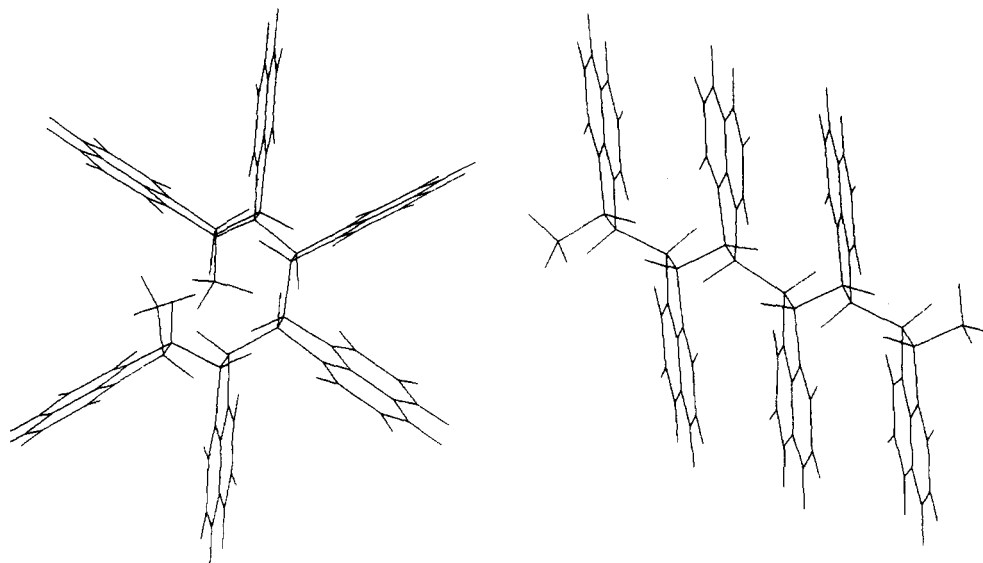
Molecular modeling of the conformations of the oligomers was performed with the aid of Sybyl version 5.2, from Tripos Associates, running on a Silicon Graphics 4D/70GT computer. The modeling simply evaluates the concentration of excimer forming sites and does not attempt to assess the extent of the population of these sites via energy migration. In the present application of this force field, the two most probable sources of error will act in opposite directions. The first source of error is performance of the calculations in a vacuum, thereby overestimating the attraction of the ring-ring interaction that would exist if the separated rings could be solvated. The second source of error is the adoption of a force field for the electronic ground state, thereby underestimating the ring-ring attraction in the presence of electronic excitation.

### Experimental Results and Discussion

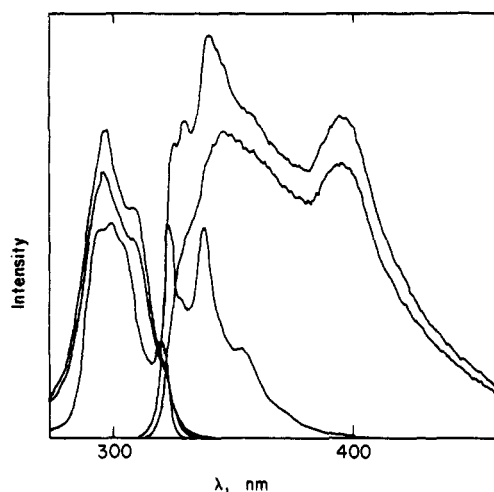
Figure 2 depicts excitation and emission spectra, measured in 1,4-dioxane, for two samples of polyacenaphthalene that were prepared by different methods, namely, thermal polymerization in the bulk and cationic polymerization in methylene chloride, using boron trifluoride triethoxide as the initiator. The shape of the excitation band is unaffected by changes in the wavelength used to monitor the emission. The emission and excitation spectra for the model compound, acenaphthene, are also depicted in Figure 2. The excitation spectrum for the model compound closely resembles that for the polymer, but the emission spectra of acenaphthene and polyacenaphthalene are quite different.

Figure 3 presents the emission spectra for acenaphthene and the two samples of polyacenaphthalene, with the intensities of the emissions normalized at 338 nm, which is the location of the maximum emission for acenaphthene. The broad band to the red of this maximum in the polymers is attributed to intramolecular excimer formation. The polymer prepared by cationic polymerization displays more intense excimer emission, but there is also strong excimer emission from the polymer prepared by thermal polymerization in the bulk. The ratio  $I_D/I_M$  will be used as a measure of the extent of excimer emission, where  $I_D$  is the intensity of the emission at the maximum at 396 nm and  $I_M$  is the intensity at 338 nm.

\* To whom correspondence should be addressed at The University of Akron.



**Figure 1.** Idealized conformations of hexamers of polyacenaphthalene with three-diisotactic (left) and three-disyndiotactic (right) stereochemical compositions. The dihedral angles in the main chain that are not part of rings are set at  $180^\circ$ , and each ring system is planar.



**Figure 2.** Fluorescence emission and excitation spectra for acenaphthene and polyacenaphthalene in 1,4-dioxane. The upper spectra are for the sample of the polymer that was prepared by thermal polymerization in the bulk, and the middle spectra are for the polymer prepared by cationic polymerization. The lowest spectra are for acenaphthene. The scales for the intensities differ for the various spectra.

The dependence of  $I_D/I_M$  on temperature for both samples of polyacenaphthalene, in three solvents, is depicted in Figure 4. In all solvents and at all temperatures,  $I_D/I_M$  is larger for the polymer with predominantly three-diisotactic stereochemical composition than for the polymer with predominantly three-disyndiotactic stereochemical composition. Measurements in all three solvents at  $25^\circ\text{C}$  give a value in the range  $1.52 \pm 0.04$  for the ratio of  $I_D/I_M$  for the three-diisotactic polymer to  $I_D/I_M$  for the three-disyndiotactic polymer. An important objective of the modeling effort will be to rationalize why the polymer with predominantly three-diisotactic stereochemical composition should have a value of  $I_D/I_M$  that is  $\sim 50\%$  larger than that observed for the polymer with predominantly three-disyndiotactic stereochemical composition.

### Molecular Modeling

**Methodology.** The molecules studied in the molecular modeling were diads, triads, tetrads, pentads, and

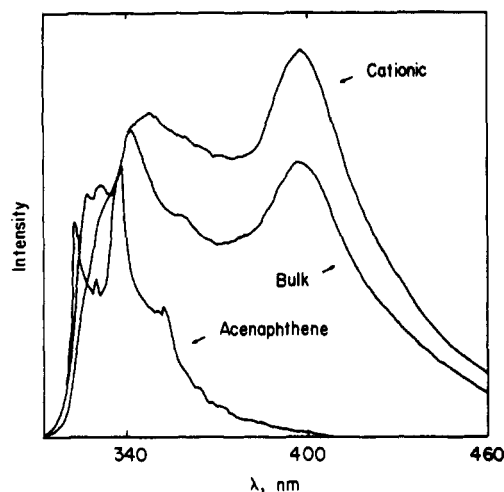


**Figure 3.** Normalized (at 338 nm) emission spectra for acenaphthene and the two samples of polyacenaphthalene in 1,2-dichloroethane at  $25^\circ\text{C}$ . Excitation is at 298 nm.

hexads of polyacenaphthalene. The number of monomer units in each oligomer is denoted by  $m$ . Each oligomer was terminated with methyl groups at both ends. The methodology was different for the molecules with two to four aromatic units than for the molecules with five or six aromatic units. A quantitative method was used for the molecules with two to four aromatic units. All local minima in the conformational energy surface were located for each molecule, and the conformation was optimized at each minimum. Bond angles and bond lengths, as well as torsional angles, were variables during the optimization. A conformational partition function was formulated for each molecule as

$$Z = \sum \exp(-E_i/RT) \quad (1)$$

where the summation extends over all of the local minima and  $E_i$  denotes the conformational energy at the  $i$ th minimum, after optimization. A value that will be taken to be proportional to the experimentally determined  $I_D/I_M$  was extracted from  $Z$  as

$$\langle p_T \rangle = \langle p_{NN} \rangle + \langle p_{N\bar{N}N} \rangle + \langle p_{N\bar{N}\bar{N}N} \rangle + \dots \quad (2)$$

where  $\langle p_{NN} \rangle$ ,  $\langle p_{N\bar{N}N} \rangle$ , etc. are proportional to the population of excimers formed by nearest neighbors, next near-

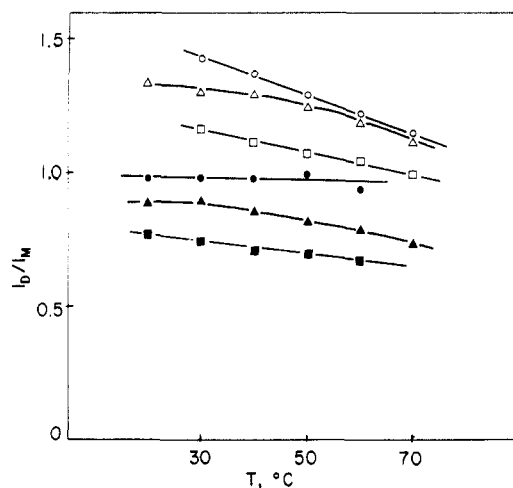


**Figure 4.** Dependence on temperature of  $I_D/I_M$  for two samples of polyacenaphthalene in three solvents. The polymers are polyacenaphthalene with stereochemical compositions that are threo-diisotactic (open symbols) and threo-disyndiotactic (filled symbols). The solvents are 1,4-dioxane (triangles), 1,2-dichloroethane (circles), and ethyl acetate (squares).

est neighbors, etc.

$$\langle p_{NN} \rangle = Z^{-1} \sum s_i \exp(-E_i/RT) \quad (3)$$

where  $s_i$  must be 0 or a small positive integer. The value of  $s_i$  is 0, 1, 2, ...,  $m-1$  if the geometry of 0, 1, 2, ...,  $m-1$  of the pairs of nearest-neighbor aromatic rings satisfy the criteria for formation of an excimer. The extension of eq 3, and the definition of  $s_i$ , to the evaluation of  $\langle p_{N_{xx}N} \rangle$ ,  $\langle p_{N_{xx}N} \rangle$ , etc., is obvious. The criteria adopted for the assignment  $s_i > 0$  were  $3 \text{ \AA} < d < 4 \text{ \AA}$  and  $0 < \psi < 30^\circ$ , where  $d$  denotes the distance between the centroids of six-membered rings on two different naphthalene groups and  $\psi$  denotes the angle between the normals of the mean planes for these two rings.

A more qualitative approach was used for the pentads and hexads because of the amount of time that would have been required for examination of all of the local minima in the conformational energy surface. Here the oligomer was initially generated in a conformation in which the two rings at the ends were in a geometry that closely approximates an excimer. This geometry had a separation of 3–4 Å for the centroids of the two rings. When this conformation was used as a starting point in an optimization, one of two results was always obtained. Either the molecule changed conformation in a way that moved the rings apart, or the conformational energy obtained after optimization was so large that the conformation would have a negligible probability. For the tetrad, both the quantitative and qualitative procedures were used, with equivalent results.

**Diads.** There are two configurational isomers, threo and erythro, of 1,2-dimethylacenaphthene. Taking these isomers into account, there are three distinct configurational isomers for each of the two methyl-terminated diads. All six of these diads were analyzed. Figure 5 depicts the two diads that are most pertinent because they have the stereochemical compositions that dominate in the two samples of polyacenaphthalene. Upon rotation about the central C–C bond, with all other parts of the structure held rigid, local minima are obtained near  $60^\circ$ ,  $200^\circ$ , and  $340^\circ$  for the threo-diisotactic diad, and near  $\pm 70^\circ$  and  $180^\circ$  for the threo-disyndiotactic diad. Optimization of the structures of the molecules, starting from each of these conformations as well as the twelve conformations for the four diads with other stereochemical configurations,

yields the conformations and conformational energies that are summarized in Table I. The optimization stops at conformations that are very close to the local energy minima, as is apparent by examination of the first two entries for threo-disyndiotactic and erythro-disyndiotactic in Table I. In each case, the symmetry of the diad argues that each pair of conformations should be mirror images and therefore they should have the same energies. As shown in Table I, the energies differ by up to 0.01 kcal/mol. The values of  $\phi_1$  also differ by a few degrees from the ideal pairs for mirror images.

Optimization produces changes in  $\phi_1$  that can be as large as  $26^\circ$ . The change in  $\phi_1$  is accompanied by changes in bond angles and distortions of each acenaphthalene unit away from planarity. Table I shows that three of the eighteen optimized structures produce an overlap of two six-membered rings in one monomer with the two six-membered rings in the other monomer. An additional three optimized structures have an overlap of one six-membered ring from one monomer with a six-membered ring from the other monomer. The distance(s) between the centroids, and the angles between the best normals to the rings, are listed in Table I for these six conformations. The last column in Table I lists the values of  $\langle p_{NN} \rangle$  that are calculated from eq 3. The three iso configurations of the dimer (threo-diisotactic, erythro-diisotactic, and threo-erythro-diisotactic) have access to excimer-forming conformations. A fourth configuration, threo-erythro-syndio, would join this list if the upper limit for  $\psi$  were raised to  $31^\circ$ . A much greater relaxation in the criteria for  $d$  and  $\psi$  would be necessary in order to place the last two configurations on the list. Overlap of both six-membered rings in one naphthalene with both six-membered rings in the other naphthalene occurs only in the three iso dimers.

One of the three configurations with large values of  $\langle p_{NN} \rangle$ , threo-diisotactic, is the dominant configuration in the sample of polyacenaphthalene that was prepared by cationic polymerization. The optimized structure with  $\phi_1 = 174^\circ$  is depicted on the right-hand side of Figure 6. The view is from a direction that is perpendicular to the central CH–CH bond and in the mean plane defined by the CH–CH–CH–CH fragment. Consequently the direction of the view is comparable with that used for the starting structure on the left-hand side of Figure 6, in which the CH–CH–CH–CH fragments were planar. Comparison of these two structures shows that, in addition to the change in  $\phi_1$ , there are distortions in the rings systems. In the starting structure, the value of  $\psi$  was  $57^\circ$ . The optimization reduces the value of  $\psi$  to  $22^\circ$ . The reduction in the value of  $\psi$  is achieved by significant distortion of the five-membered ring. (The value of the  $C^{ar}$ –CH–CH– $C^{ar}$  angle in the five-membered ring is  $22^\circ$  in the optimized structure.) Recent work with poly(*p*-tert-butylstyrene) shows that excimer emission can be observed in such a system when  $\psi$  is as large as  $22^\circ$ .<sup>12</sup> On this basis, we conclude that nearest-neighbor naphthalene rings can form an excimer in polyacenaphthalene.

The conclusion to the contrary that has appeared in the literature<sup>2–6</sup> seems to have been based on consideration of structures that were not subjected to a full valence optimization. It is this optimization that converts the structure on the left-hand side of Figure 6 to the structure on the right-hand side. This conclusion is reinforced upon analysis of the structure by using molecular dynamics. Over a time period on the order of 10 ps, the value of  $\psi$  fluctuates over the range  $0$ – $30^\circ$  and the values of  $d$  fluctuate from 3.2 to 4.3 Å. Thus the fluctua-

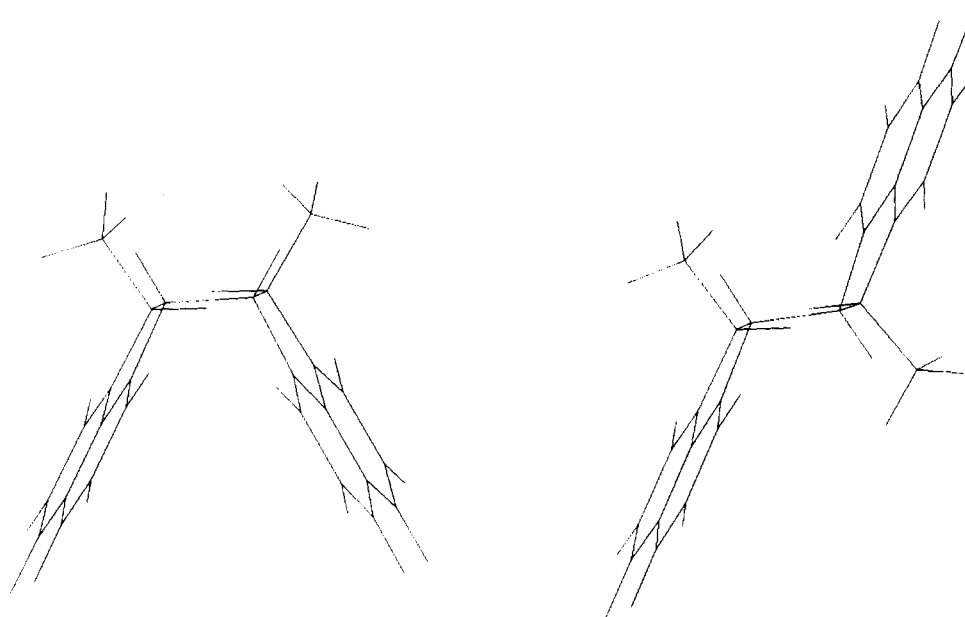


**Figure 5.** Structures, before optimization, of the threo-diisotactic (left) and threo-disyndiotactic (right) diads, each methyl terminated and with a dihedral angle of 180° for the bond between the two rings. The view of each diad is perpendicular to the central CH-CH bond.

**Table I**  
Optimized Structures and Conformational Energies for Methyl Terminated Diads

diad <sup>a</sup>	$\phi_1$ , <sup>b</sup> deg		$E_i$ , <sup>c</sup>	over- lap <sup>d</sup>	$d$ , <sup>e</sup>	$\psi$ , <sup>f</sup> deg	$\langle p_{NN} \rangle$
	start	end					
t-diiso (XXXX)	200	174	17.96	2	3.36–3.38	22	0.85
	60	61	18.98				
	335	338	26.85				
t-disyndio (XXOO)	295	296	18.62	1	4.60	44	0.00
	70	64	18.63	1	4.60	44	
	180	180	24.56				
e-diiso (XOOX)	170	175	24.14	2	3.17–3.42	12	0.98
	305	296	26.44				
	85	89	27.96				
e-disyndio (XOOX)	65	67	25.17				0.00
	300	294	25.17				
	180	185	29.32				
te-iso (XXOX)	195	182	21.37	2	3.43–3.43	20	0.63
	60	58	21.72				
	280	271	23.77				
te-syndio (XOOX)	290	293	20.37	1	3.88	31	0.00
	65	61	22.30				
	195	192	28.29				

<sup>a</sup> The terminology for the stereochemistry is from Huggins et al.<sup>7</sup> As an example, t-diiso denotes threo-diisotactic, in which the four hydrogen atoms in the CH groups are on the same side, as denoted by the XXXX in parentheses. In t-disyndio the first two hydrogen atoms are on one side and the last two on the other side, as denoted by the XXOO in parentheses. <sup>b</sup> Initial and final values of  $\phi_1$  in the optimization. <sup>c</sup> Energy (kcal/mol) after optimization. <sup>d</sup> Number of pairs of six-membered rings that overlap in the optimized conformation. <sup>e</sup> Separation of the centroids of the rings cited in the previous column. <sup>f</sup> Angle between the normals to the best planes through the rings, for those cases where there is an entry in the preceding two columns.

tions anticipated in the structure at ordinary temperatures are sufficient to cause it to visit a classic excimer-forming conformation several times in a nanosecond.

The configuration that is dominant in the polyacenaphthalene prepared by bulk thermal polymerization, i.e., threo-disyndiotactic, has a value of 0 for  $\langle p_{NN} \rangle$ . The entries in Table I for this configuration show that substantial relaxation in the criteria for both  $d$  and  $\psi$  would be necessary in order to produce a nonzero value for  $\langle p_{NN} \rangle$ .

**Triads.** The only two triads studied were those that have the stereochemical compositions that are dominant

in the two samples of polyacenaphthalene that were studied by fluorescence. Nine local minima were found in the conformational energy surface for each of these triads. The torsional angles  $\phi_1$  and  $\phi_2$  at the minima are near the values expected from the study of the corresponding dyads. Each of these structures was subjected to a full valence optimization. The results are presented in Table II. For the iso triads, three starting conformations ( $\phi_1, \phi_2 = 60^\circ, 60^\circ; 60^\circ, 335^\circ; 335^\circ, 60^\circ$ ) produce the same structure upon optimization ( $\phi_1, \phi_2 = \sim 50^\circ, 50^\circ$ ). This conformation brings the terminal naphthalene rings into a close approximation to an excimer-forming geometry, as shown in Figure 7. The value of  $\langle p_{NN} \rangle$  in Table II is  $Z^{-1} \exp(-E_i/RT)$ , with  $E_i$  being the optimized energy for this conformation. Another conformation of higher probability brings nearest-neighbor rings into an excimer-forming geometry. This conformation, which is depicted in Figure 8, has a conformation for each diad that is closely related to the excimer-forming conformation for threo-diisotactic in Table I. The value of  $\langle p_{NN} \rangle$  for this structure in Table II is  $2Z^{-1} \exp(-E_i/RT)$ , where  $E_i$  is the optimized energy of this conformation, and the factor 2 arises because there are two pairs of excimers in this structure. No other structures of the iso triad merit the listing of a numerical value of  $\langle p_{NN} \rangle$  or  $\langle p_{NNN} \rangle$  in Table II because either  $s_i$  is zero or  $Z^{-1} \exp(-E_i/RT)$  is very small.

The syndio triad is especially interesting because it fulfills the criteria for a nearest-neighbor excimer, even though the threo-disyndiotactic diad did not, as was shown in Table I. The optimized structure of lowest energy, and with acceptable excimer-forming geometry, in the triad has  $\phi_1, \phi_2 = 293^\circ, 298^\circ$ , which are only slightly different from the value of  $\phi_1, 296^\circ$ , in the optimized structure of the diad. These slight changes in  $\phi$ , as well as other small distortions in the interior monomer unit, are sufficient to decrease  $\psi$  from  $44^\circ$  to  $\sim 27^\circ$  and to decrease  $d$  from 4.60 to  $\sim 3.7$  Å.

**Tetrads.** As expected from the behavior of the diad and the triad, the starting conformation  $\phi_1 = \phi_2 = \phi_3 = 200^\circ$  converges upon optimization to a conformation in which nearest-neighbor rings are in an environment conducive to excimer formation. This conformation has  $\phi_1$ ,

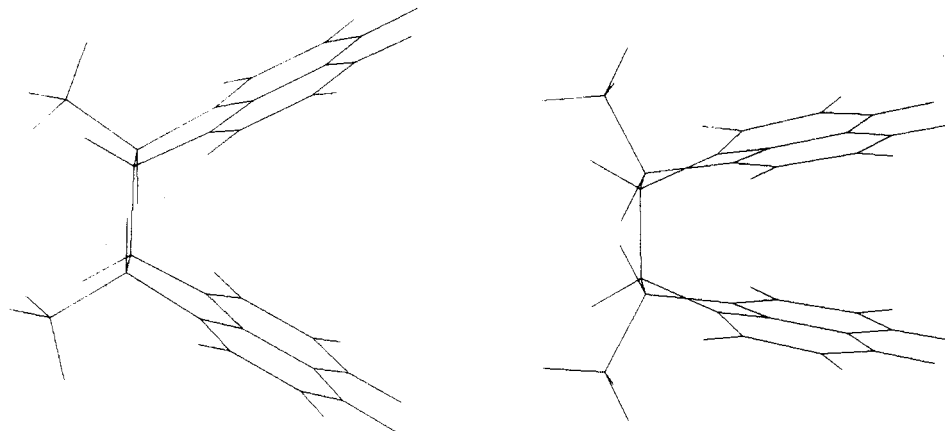


**Figure 6.** Optimized structure (right) of the methyl-terminated threo-diisotactic diad with  $\phi_1 = 174^\circ$ , obtained starting from the structure on the left. The view is from a direction perpendicular to the central CH-CH bond and nearly in the mean plane defined by the CH-CH-CH-CH bonds.

**Table II**  
Optimized Structures of Two Methyl-Terminated Triads

$\phi_1, \phi_2$		$E_i$	type	overlap	$d, \text{\AA}$	$\psi, \text{deg}$	$\langle p_{NN} \rangle$	$\langle p_{N \times N} \rangle$
start	end							
Iso Triad								
200, 200	172, 173	23.54	NN	2	3.32–3.37	24	1.57	
				2	3.36–4.33	22		
60, 60	51, 51 <sup>a</sup>	24.32	NxN	1	3.70	17		0.21
60, 335	51, 50 <sup>a</sup>	24.32	NxN	1	3.70	14		0.21
335, 60	50, 50 <sup>a</sup>	24.32	NxN	1	3.70	14		0.21
60, 200	60, 201	27.28	NN	1	3.98	50		
200, 60	200, 61	27.28	NN	1	3.98	49		
335, 200	337, 205	35.95	NxN	1	3.70	55		
200, 335	205, 338	35.96	NxN	1	3.70	55		
335, 335	343, 344	39.36	NxN	1	5.30	high		
Syndio Triad								
295, 70	297, 64	25.49	NN	1	4.41	47		
					4.34	45		
70, 295	64, 297	25.52	NN	1	4.41	46		
					4.61	47		
295, 285	293, 298	25.53	NN	1	3.66	29	0.5	
					3.73	27		
70, 70	64, 64	25.84	NN	1	4.38	45		
					4.37	46		
180, 295	181, 296	29.68	NN	1	3.96	33		
295, 180	295, 177	29.70	NN	1	4.14	34		
70, 180	69, 204	30.10						
180, 180	201, 201	30.18	NN	1	3.30	11		
180, 70	161, 62	30.31	NN	1	4.06	40		

<sup>a</sup> This optimized conformation is obtained from three different starting conformations. It is counted only once in the evaluation of  $\langle p_{N \times N} \rangle$ .

$\phi_2, \phi_3 = 171^\circ, 170^\circ, 171^\circ$ . Its value of  $3Z^{-1} \exp(-E_i/RT)$  is 1.17. Three of the starting conformations of the isotetrad,  $\phi_1, \phi_2, \phi_3 = (60^\circ, 60^\circ, 60^\circ)$ ,  $(60^\circ, 60^\circ, 335^\circ)$ , and  $(335^\circ, 60^\circ, 335^\circ)$ , converge to the  $\phi_1, \phi_2, \phi_3 = 51^\circ, 45^\circ, 51^\circ$  upon optimization. This optimized conformation has a next-to-nearest neighbor excimer forming environment for each of the two pairs. The value of  $2Z^{-1} \exp(-E_i/RT)$  is 1.11. Only one other conformation contributes significantly to the excimer population in this tetrad, and its contribution is small. That conformation, after optimization, is  $\phi_1, \phi_2, \phi_3 = 50^\circ, 49^\circ, 177^\circ$ . It contributes a value of 0.04 to both  $\langle p_{NN} \rangle$  and  $\langle p_{N \times N} \rangle$ . For all conformations, the totals for  $\langle p_{NN} \rangle$  and  $\langle p_{N \times N} \rangle$  are 1.21 and 1.16, respectively. None of the optimized conformations bring the two terminal naphthalene rings into an excimer-forming conformation, and therefore  $\langle p_{N \times N} \rangle = 0.00$ .

The most important excimer-forming conformations in the syndio tetrad are the ones that would have been pre-

dicted on the basis of the result for the triad. The optimized conformations are  $\phi_1, \phi_2, \phi_3 = 65^\circ, 65^\circ, 296^\circ$  and  $64^\circ, 297^\circ, 297^\circ$ . The first structure has one set of nearest-neighbor excimers, which involve the first two monomer units, and the second conformation has two sets of nearest-neighbor excimers, involving the last three monomer units. (The first conformation would contribute a second nearest-neighbor excimer if the upper limit for  $\psi$  were  $31^\circ$ .) Another conformation,  $296^\circ, 297^\circ, 296^\circ$ , contributes a small value of  $\langle p_{NN} \rangle$ . When evaluated for all conformations,  $\langle p_T \rangle$  has the value of 1.08. The values of  $\langle p_{N \times N} \rangle$  and  $\langle p_{N \times N \times N} \rangle$  are 0.00, the former because the conformations that produce next-to-nearest neighbor excimers have high energies and the latter because none of the conformations bring the two terminal naphthalene rings into an excimer-forming geometry.

**Pentads and Hexads.** Investigation of the pentads and hexads identifies the nearest-neighbor and next-to-nearest neighbor excimers that would have been expected

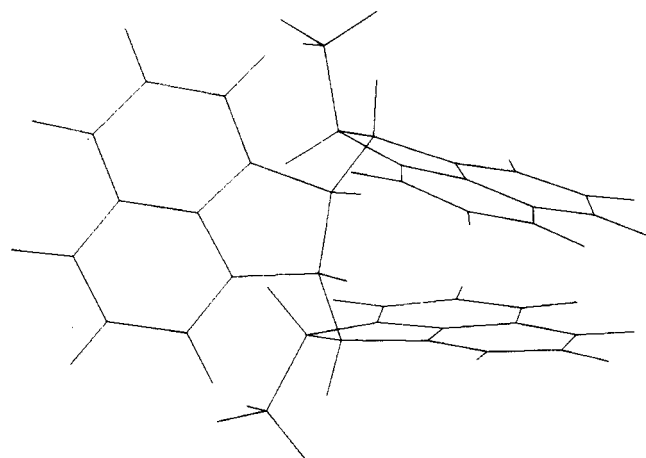


Figure 7. Optimized structure of the methyl terminated iso triad with  $\phi_1 = \phi_2 = 50^\circ$ , showing the relationship between the ring systems in the two terminal units.

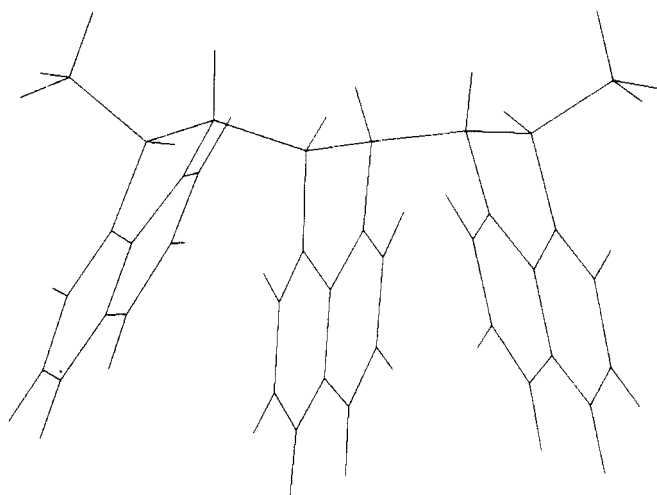


Figure 8. Optimized structure of the methyl terminated iso triad with  $\phi_1, \phi_2 = 172^\circ, 173^\circ$ .

Table III

Summary of the Calculations of  $\langle p_{NN} \rangle$ ,  $\langle p_{N \times N} \rangle$ , and  $\langle p_{N \times \times N} \rangle$

stereochemistry	oligomer	$\langle p_{NN} \rangle$	$\langle p_{N \times N} \rangle$	$\langle p_{N \times \times N} \rangle$	$\langle p_T \rangle$
iso	diad	0.85			0.85
	triad	1.57	0.21		1.18
	tetrad	1.21	1.16	0.00	2.37
syndio	diad	0.00			0.00
	triad	0.55	0.00		0.54
	tetrad	1.08	0.00	0.00	1.08

from the analysis of the diads and triads, and no additional species of any significance. Thus  $\langle p_{NN} \rangle > 0$  and  $\langle p_{N \times N} \rangle > 0$ , but  $\langle p_{N \times \times N} \rangle = \langle p_{N \times \times \times N} \rangle = \langle p_{N \times \times \times \times N} \rangle = 0.00$ .

## Discussion

Table III summarizes the values of  $\langle p_{NN} \rangle$ ,  $\langle p_{N \times N} \rangle$ , and  $\langle p_{N \times \times N} \rangle$  for the iso and syndio compounds, as well as their sum, denoted by  $\langle p_T \rangle$ . It is of interest to compare these results with the experimental observation that  $I_D/I_M$  is  $\sim 50\%$  larger for the polyacenaphthalene with predominantly threo-diisotactic stereochemistry than for the polyacenaphthalene with predominantly threo-disyndiotactic stereochemistry. That comparison is presented graphically in Figure 9. For both stereochemistries,  $\langle p_T \rangle$  increases as the size of the oligomer increases. Although the extrapolation is a long one and requires the assumption that  $\langle p_T \rangle$  is linear in  $1/m$  the behavior of a polymer of high molecular weight can be predicted by linear

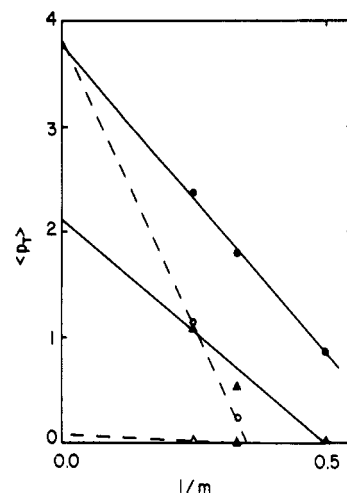


Figure 9.  $\langle p_T \rangle$  for iso (filled circles) and syndio stereochemistry (filled triangles), as a function of  $1/m$ , where  $m$  denotes the number of naphthalene units in the oligomer. Open circles and triangles depict the results that would have been obtained if  $\langle p_{NN} \rangle$  were set equal to zero in all cases. The solid lines are drawn through the filled symbols, and the dashed line is drawn through the open symbols.

extrapolation of the three points in each series. This linear extrapolation amounts to the assumption that the only excimers that are important in the polymer are the ones that can be identified in the oligomers that were subjected to conformational analysis and that the increase in the degree of polymerization does not alter the local conformation in any important way. The ratio of  $\langle p_T \rangle$  for the iso polymer to the value of  $\langle p_T \rangle$  for the syndio polymer is infinite at  $m = 2$  has fallen to 2.2 at  $m = 4$  and, by extrapolation of the two solid lines in Figure 9, approaches a value of about 1.8 as  $m$  becomes infinite. This ratio is not too different from the value of 1.5, which is the ratio of  $I_D/I_M$  obtained from the fluorescence of the two samples of polyacenaphthalene.

If we were to arbitrarily reject the possibility of a nearest-neighbor excimer in polyacenaphthalene, i.e., arbitrarily set  $\langle p_{NN} \rangle = 0$ , the analysis would have produced the open symbols and the dashed lines in Figure 9. This analysis is equivalent to one in which the only excimers are assumed to be those formed between next-to-nearest neighbors. The ratio of  $\langle p_T \rangle$  for the two stereochemistries is large at both  $m = 3$  and  $m = 4$ . Although the dashed linear extrapolations are based on only two points, provided by the open symbols at  $m = 3$  and 4, they show quite unambiguously that the values of  $\langle p_T \rangle$  remain different at larger values of  $m$ . Clearly the observations that the values of  $I_D/I_M$  for the two polyacenaphthalene samples vary by only 50% cannot be rationalized by next-to-nearest excimers alone. Successful rationalization of the experimental results requires incorporation in the analysis of the nearest-neighbor excimers that are identified in the molecular modeling study.

**Acknowledgment.** This research was supported by National Science Foundation Grant DMR 87-06166, by the Ohio Board of Regents under its Research Challenge, and by Comunidad de Madrid and CICYT PB88-0152 (Spain).

## References and Notes

- (1) Schneider, F.; Springer, J. *Makromol. Chem.* **1971**, *146*, 181.
- (2) David, C.; Lempereur, M.; Geuskens, G. *Eur. Polym. J.* **1972**, *8*, 417.
- (3) David, C.; Piens, M.; Geuskens, G. *Eur. Polym. J.* **1972**, *8*, 1019.
- (4) Wang, Y.-C.; Morawetz, H. *Makromol. Chem. Suppl.* **1975**, *1*, 283.

- (5) Phillips, D.; Roberts, A. J.; Soutar, I. J. *Polym. Sci., Polym. Lett. Ed.* **1980**, *18*, 123.
- (6) Reid, R. F.; Soutar, I. J. *Polym. Sci., Polym. Phys. Ed.* **1980**, *18*, 457.
- (7) Braun, H.; Forster, Th. *Ber. Bunsen-Ges. Phys. Chem.* **1966**, *70*, 1091.
- (8) Story, V. M.; Canty, G. J. *Res. Natl. Bur. Stand.* **1964**, *68A*, 165.
- (9) Tsvetkov, V. N.; Vitovskaya, M. G.; Lavrenko, P. N.; Zakharova, E. N.; Gavrilenko, I. F.; Stevanovskaya, N. N. *Polym. Sci. USSR (Engl. Transl.)* **1971**, *11*, 2845.
- (10) Chu, E. Ph.D. Dissertation, The University of Akron, 1987.
- (11) Higgins, M. L.; Natta, G.; Desreux, V.; Mark, H. *Makromol. Chem.* **1965**, *82*, 1.
- (12) Chakraborty, D.; Heitzhaus, K. D.; Hamilton, F. J.; Harwood, H. J.; Mattice, W. L. Submitted for publication.

## Effect of Hydrostatic Pressure on Local Polymer Dynamics in Poly(propylene oxide)

Benny D. Freeman,<sup>†</sup> Liliane Bokobza,\* Philippe Sergot, and Lucien Monnerie

*Laboratoire de Physico-Chimie Structurale et Macromoléculaire, Ecole Supérieure de Physique et de Chimie Industrielles de la Ville de Paris, 10 rue Vauquelin, 75231 Paris, Cedex 05, France.*

F. C. De Schryver

*Department of Chemistry, University of Leuven, Celestijnenlaan 200F, B-3030 Heverlee, Belgium. Received July 21, 1989; Revised Manuscript Received October 25, 1989*

**ABSTRACT:** The effect of hydrostatic pressure on the local molecular motion in bulk polymers has been studied by measuring the pressure dependence of the fluorescence lifetime of the intramolecular excimer-forming probe molecule *meso*-2,4-di-*N*-carbazolylpentane dissolved in poly(propylene oxide) of molecular weights 425, 2000, and 4000. The experiments were performed at 313 K and covered a pressure range of 1–3000 bar. The experimental data are compared with the predictions of several free volume based models of polymer dynamics and with previous dipole relaxation measurements of poly(propylene oxide) dynamics.

### Introduction

Local- or molecular-scale motions in bulk polymers near the glass-rubber transition temperature have a strong influence on many polymer properties. These local-scale polymer chain motions may be studied by measuring the dynamics of intramolecular excimer-forming probes dispersed in polymer matrices.<sup>1–9</sup> Intramolecular excimers are usually formed in bichromophoric molecules whenever the two aromatic chromophores are separated by a three-atom linkage.<sup>10</sup> When one of the chromophores is electronically excited and the molecule undergoes a rotation about the three-atom linkage, which brings the two aromatic groups into a sandwichlike conformation where the  $\pi$  electronic orbitals overlap, the electrons in the excited and unexcited chromophores may interact to produce a stable excimer conformation. When the mobility of the environment surrounding the fluorescent molecule controls the rate of this intramolecular rotational motion, then the fluorescence lifetime of the excited chromophore (that is, the time for the chromophore to relax from the excited state back to the ground state) will be sensitive to the media mobility. Because the motion of the chromophore to reach the excimer conformation is well-defined, the volume swept out during the motion

may be calculated. Therefore, this technique provides a unique method for probing the state of free volume in the fluorescent molecule's environment. The probe molecule can also be changed; thus, the volume required to reach the excimer conformation is changed. This extra degree of freedom permits quantitative access to the availability of free volume for molecular-scale motion of a fixed size on a time scale of the fluorescent lifetime of the probe molecule.

The temperature dependence of polymer dynamics has been studied by many different techniques and is generally well-understood. However, the effect of hydrostatic pressure on chain dynamics is still poorly understood. The effect of temperature and hydrostatic pressure on the dipole relaxation in poly(propylene oxide) has been measured by Williams.<sup>11</sup> This work showed that the time-temperature superposition principle was obeyed by this polymer at all experimental conditions, that the temperature dependence of the frequency of maximum dielectric loss,  $f_{\max}$ , was consistent with the predictions of the WLF equation,<sup>12</sup> but that the pressure dependence of  $f_{\max}$  was not consistent with predictions of the extension of the WLF equation to high pressure. In another study, the effect of temperature on the dynamics of excimer-forming probe molecules dispersed in poly(propylene oxide) has been measured.<sup>8</sup> This study indicated that the excimer dynamics probed the local scale polymer dynamics and that the results were consistent with the WLF equa-

\* To whom correspondence should be addressed.

<sup>†</sup> Permanent address: Department of Chemical Engineering, North Carolina State University, Raleigh, NC 27615.